International Journal of Offshore and Polar Engineering (ISSN 1053-5381)

Vol. 27, No. 2, June 2017, pp. 177–183; https://doi.org/10.17736/ijope.2017.as19

http://www.isope.org/publications/publications.htm

# On the Tidal Resonance of the Bristol Channel

Chanshu Gao and Thomas A. A. Adcock
Department of Engineering Science, University of Oxford
Oxford, Oxfordshire, United Kingdom

**The Bristol Channel has one of the largest tidal ranges in the world. A key cause for this is the resonance with the dominant semidiurnal tides. In this paper we use numerical simulations to investigate this resonance. We first vary the frequency on the boundary of the model and examine at which frequency the model is excited. Second, we apply a disturbance to the model and analyse the frequency at which it resonates. We examine the sensitivity of these results, finding them sensitive to the bed friction used (with possible implications for energy extraction) but insensitive to small changes in the tidal amplitude on the boundary or the mean-water level.**

## INTRODUCTION

The Bristol Channel and Severn Estuary constitute one of the largest, semienclosed water basins in the United Kingdom. The Bristol Channel is located in the southwest coast of Great Britain. The Severn Estuary is situated at the upper reaches of the Bristol Channel, which has the second-largest semidiurnal tidal ranges worldwide. The typical mean spring tidal range is 12.2 m, with the high spring tidal range approaching 14 m at the Severn mouth. The large tidal ranges observed in the Bristol Channel and the Severn Estuary are driven by two main mechanisms (Robinson, 1980; Xia et al., 2012; Serhadlıoğlu, 2014). One is the funnelling effect at the upper reaches of the Bristol Channel due to its wedge-shaped geometry and shallow bathymetry. However, it has long been pointed out by Marmer (1922) that this effect is not enough to produce the observed tidal range. The other mechanism is the quarter wavelength resonance of the Bristol Channel with the incident North Atlantic tidal wave (Fong and Heaps, 1978).

Despite a number of previous model studies having been undertaken for the Bristol Channel, its complex hydrodynamic system is not yet fully understood, particularly given its resonant nature. Resonant systems are typically very sensitive to small changes, and these responses are highly site dependent (Adcock et al., 2015). In this study we seek to improve the understanding of the resonance in the Bristol Channel. A simplified 2-D model has been developed from the model of Serhadlıoğlu et al. (2013) to investigate the resonances in the Bristol Channel.

In this paper, the model equations and the model parameters used for the Bristol Channel region are first considered. Then, the model is tested by comparing its results with previous model studies and observations. Two methods have been used to determine the resonant periods of the Bristol Channel. A frequency sweep is used by varying the forcing frequency on the open boundary of the model to find the peak response of the semidiurnal tidal amplitude. Next, the key properties that influence the resonances are investigated. Finally, wind disturbances are applied to examine the oscillation periods of surge response.

Received June 17, 2016; updated and further revised manuscript received by the editors December 30, 2016. The original version (prior to the final updated and revised manuscript) was presented at the Twenty-sixth International Ocean and Polar Engineering Conference (ISOPE-2016), Rhodes, Greece, June 26–July 1, 2016.

KEY WORDS: ADCIRC, tidal resonance, shallow-water equations, numerical modelling, Bristol Channel.

## RELATED WORK

Systems that are forced by oscillations close to their natural period have large amplitude responses. This phenomenon is called resonance (Pugh, 1996). In oceanography, a tidal resonance occurs when the tide excites one of the resonant modes of the ocean. This occurs when a continental shelf is about a quarter wavelength wide. The whole global ocean system seems to be near resonance at semidiurnal tidal frequencies, and the observed tides are substantially larger than the equilibrium tide (Baker, 1991; Pugh and Woodworth, 2014).

In some studies, the phenomenon of quarter-wavelength resonance was explained by standing wave theory (Pugh, 1996; Pugh and Woodworth, 2014). Consider the simplest case of a wave travelling in a long channel being reflected without loss of amplitude at a closed end. The superposition of incident and reflected waves can resemble a standing wave; standing waves have alternate nodes, positions where the amplitude is zero, and antinodes, positions where the amplitude is a maximum, each separated by a distance of $\lambda/4$ where $\lambda$ is the wavelength of the original progressive wave (Pugh, 1996). A model of an open box approximates to the tidal behavior of many shelf sea basins (Pugh, 1996). If we describe the movement of water in a box whose length is a quarter wavelength with one closed end and one open end, and the water is driven by oscillatory in and out currents at the open end, then the open end is at the first node and currents at the entrance could produce large changes of level at the head. Although exact quarter-wave dimension would be very unlikely, the possibility of tidal amplification still exists.

### Model Setup

The model was built from Serhadlıoğlu's study (Serhadlıoğlu, 2014) whose modelling region includes the Irish Sea, the Celtic Sea and the Bristol Channel. An unstructured mesh was developed by the ADvanced CIRCulation model (ADCIRC) with Surface-water Modelling System (SMS). A mesh convergence study has been conducted to evaluate the necessary level of resolution required in the numerical model to obtain a converged $M_2$ response using five unstructured triangular finite element meshes (Serhadlıoğlu, 2014). On the open boundary, the water depths were prescribed and were the best estimates based on previous work (Serhadlıoğlu et al., 2013), and no current was specified on the boundary.

As seen in Fig. 1, the model domain stretches from the outer Bristol Channel, close to Lundy Island, to Caldicot and thereby

| References | Comment | Areas included | Friction coefficient | Fundamental period (hours) | $\omega/\omega_{M_2}$ |
|---|---|---|---|---|---|
| Fong and Heaps (1978) | 1-D numerical model to investigate the quarter-wave tidal resonance in the Bristol Channel – Celtic Sea shelf area | Celtic Sea and Bristol Channel | Not included | Celtic Sea: 12.2–12.6 | 0.98–1.02 |
| Heaths (1981) | A linear resonant model fitted to the semi-diurnal tidal constituents | Celtic Sea, Bristol Channel and the southern Irish Sea | N/A | Celtic Sea: 10.8–11.1 Bristol Channel: 7.3–9.0 | Celtic Sea: 1.12–1.15; Bristol Channel: 1.38–1.7 |
| Liang et al. (2014) | 1-D computational model to predict the response tidal characteristics | Severn Estuary and Bristol Channel | Roughness height: 35 mm (same as in Falconer, 2009) | Bristol Channel: 8–9 | 1.38–1.55 |
| Serhadlıoğlu (2014) | 2-D unstructured computational model to investigate the resonance of the system | European continental shelf, Irish Sea, Celtic Sea and Bristol Channel | 0.0025 | Bristol Channel: 10.3–11.3 | 1.1–1.2 |

Table 1 Estimates of the fundamental resonant period of the Bristol Channel and the Celtic Sea derived from various theoretical models (extended table taken from Serhadlıoğlu, 2014). $\omega/\omega_{M_2}$ is the ratio between the tidal forcing frequency of the dominant resonant mode and the frequency of the $M_2$ tide.

includes the entire expanse of water from the open sea to the tidal limit. The domain is approximately 160 km long, narrowing down dramatically toward the head of the Severn Estuary, from approximately 112 km at the seaward boundary to approximately 1.4 km at the landward boundary. The coastline is permitted to inundate more than 6 m above sea level, and the water depth ranges from −65 m to +9 m from the seaward boundary to the riverine boundary.

The model domain was divided into 14,606 unstructured triangular cells and allows a large variation in the scales of regions of interest, which in this study vary from 500 m to 5,000 m. Five stations (Avonmouth, Newport, Hinkley Point, Mumbles, and Ilfracombe) were chosen as the model stations.

The resonances in the Bristol Channel have practical significance and theoretical interest. Tidal power barrages in the Severn Estuary and Bristol Channel were studied intensively in the 1980s by a UK government committee chaired by Bondi (1981). The

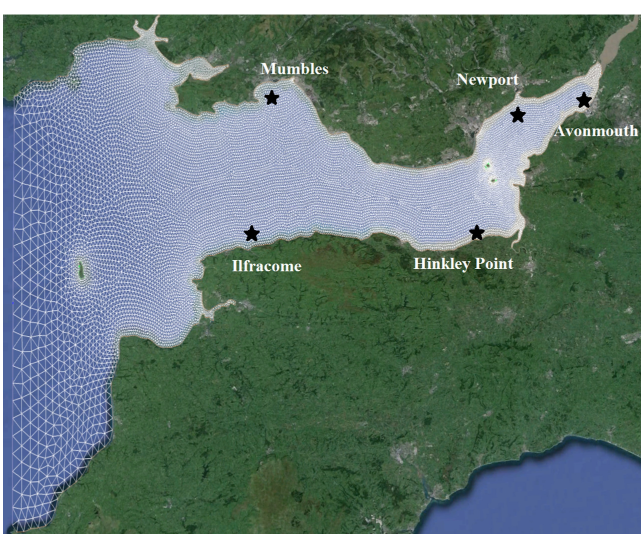


Fig. 1 Model mesh shown in Google Earth (Google Earth, 2016)

suitability of tidal stream turbine deployment sites in Wales along the Bristol Channel has also been studied by Willis et al. (2010). The tidal lagoon project in the vicinity of the Port of Swansea, South Wales, was developed in 2011 and will be started on site in approximately 2018. Therefore, to assess how these might alter the tidal characteristics of the area it is obviously important to understand the tidal dynamics as they presently exist (Fong and Heaps, 1978).

The Bristol Channel and Severn Estuary has been of particular interest to engineers and scientists for this reason, and several studies have been undertaken over the past 30 years or so. Serhadlıoğlu (2014) has worked on the resonance in the Bristol Channel using a 2-D unstructured triangular model mesh, which was the one that the present study built on. The model domain includes the Irish Sea, the Celtic Sea, the English Channel, and the Bristol Channel. In Serhadlıoğlu's study (Serhadlıoğlu, 2014), the model was excited with a single tidal component with the amplitude of the $M_2$ tide (principal lunar semidiurnal constituent) but with the frequency varied, and a resonant period of 10.3–11.3 hours was found.

## METHOD

### Shallow-Water Equations

A simplification can be made by integrating the horizontal velocity over the vertical direction to obtain a representative velocity flow field that satisfies the shallow-water equations. The 2-D shallow-water equations consist of the depth-averaged continuity equation and the $x$ and $y$ momentum equations written here in conservative form:

$$\frac{\partial \zeta}{\partial x} + \frac{\partial}{\partial x}(Hu) + \frac{\partial}{\partial y}(Hv) = 0 \tag{1}$$

$$\frac{\partial}{\partial t}(uH) + \frac{\partial}{\partial x}\left(Hu^2 + \frac{1}{2}g(H^2 - h^2)\right) + \frac{\partial}{\partial y}(Huv) = g\zeta\frac{\partial h}{\partial x} + F_x \tag{2}$$

$$\frac{\partial}{\partial t}(vH) + \frac{\partial}{\partial x}(Huv) + \frac{\partial}{\partial y}\left(Hv^2 + \frac{1}{2}g(H^2 - h^2)\right) = g\zeta\frac{\partial h}{\partial y} + F_y \tag{3}$$

| Station | $M_2$ Amplitude (m) | | | | | $M_2$ Phase (°) | | | | |
|---|---|---|---|---|---|---|---|---|---|---|
| | Obs. | $c_d(1)$ | $c_d(2)$ | $c_d(3)$ | $c_d(4)$ | Obs. | $c_d(1)$ | $c_d(2)$ | $c_d(3)$ | $c_d(4)$ |
| Stackpole Quay (51.63,4.85) | 2.51 | 2.52 | 2.52 | 2.51 | 2.51 | 168 | 172 | 172 | 172 | 172 |
| Mumbles (51.57,4) | 3.18 | 3.10 | 3.05 | 3.04 | 3.01 | 171 | 173 | 176 | 176 | 178 |
| Swansea (51.62,3.93) | 3.19 | 3.15 | 3.12 | 3.10 | 3.03 | 173 | 174 | 176 | 177 | 179 |
| Port Talbot (51.58,3.78) | 3.13 | 3.17 | 3.15 | 3.12 | 3.07 | 173 | 174 | 176 | 177 | 179 |
| Barry (51.4,3.28) | 3.92 | 3.90 | 3.80 | 3.74 | 3.62 | 185 | 182 | 188 | 190 | 193 |
| Steep Holm Island (51.33,3.1) | 3.87 | 4.04 | 3.94 | 3.88 | 3.75 | 186 | 183 | 189 | 191 | 196 |
| Cardiff (51.48,3.17) | 4.01 | 4.07 | 3.95 | 3.89 | 3.79 | 191 | 186 | 190 | 193 | 199 |
| Weston-Super-Mare (51.35,2.97) | 3.95 | 4.17 | 4.01 | 4.00 | 3.87 | 181 | 184 | 189 | 193 | 199 |
| Hinkley Point (51.2,3.13) | 3.8 | 4.00 | 3.89 | 3.83 | 3.71 | 195 | 181 | 186 | 188 | 193 |
| Minehead (51.2,3.47) | 3.59 | 3.70 | 3.64 | 3.59 | 3.49 | 183 | 176 | 180 | 182 | 186 |
| Porlock Bay (51.22,3.6) | 3.42 | 3.54 | 3.47 | 3.43 | 3.36 | 179 | 173 | 176 | 178 | 181 |
| Ilfracombe (51.2,4.12) | 3.04 | 3.00 | 2.99 | 2.97 | 2.94 | 162 | 165 | 166 | 167 | 168 |
| Appledore (51.05,4.18) | 2.57 | 2.62 | 2.59 | 2.57 | 2.52 | 165 | 170 | 172 | 173 | 174 |
| Port Isaac (50.58,4.82) | 2.47 | 2.42 | 2.42 | 2.42 | 2.41 | 144 | 151 | 151 | 151 | 151 |

Table 2 Comparison of the observed $M_2$ tidal elevations and phases against model results using various bed friction coefficients: $c_d(1) = 0.0025$; $c_d(2) = 0.0035$; $c_d(3) = 0.004$; $c_d(4) = 0.005$. The values highlighted in grey are the ones that are closer to the observations in the case of amplitude and closer to the observations with a 5° shift in the case of phase.

where $H$ is the total depth of the water column ($H = h + \zeta$), which is equivalent to the sum of the free-surface elevation ($\zeta$) and the bathymetric depth. The variables $u$ and $v$ represent the depth-averaged velocity components in the $x$ and $y$ directions. $g$ is the gravitational acceleration. $F_x$ and $F_y$ represent additional terms; in this study they represent Coriolis term, bed friction and wind shear stress. Because of the large tidal range and relatively small river discharge, the flow in the Severn Estuary and Bristol Channel does not display any significant stratification, which justifies the use of the shallow-water equations in the hydrodynamic analyses (Liang et al., 2014).

The discontinuous Galerkin methods (DG methods) are a class of finite element methods that make use of the same function space as the continuous method, but with relaxed continuity at interelement boundaries (Kubatko et al., 2006). In this study, the shallow-water equations were solved using the DG methods version of ADCIRC, which is a well-developed hydrodynamic finite element model. ADCIRC is widely used for tide and surge modelling and is in constant development, with work ongoing in the areas of adaptive grids, 3-D modelling, sediment transport, and biological processes (Kubatko et al., 2006).

From tidal analysis, the dominant constituent in the Bristol Channel is the $M_2$, followed by the $S_2$ (principal solar semidiurnal constituent), $N_2$ (larger lunar elliptic semidiurnal constituent), and $\mu_2$ (variational semidiurnal constituent) (Hashemi et al., 2008), but in this study attention is restricted to the dominant harmonic constituent, the $M_2$ tide. The ocean boundary was forced with a single sinusoidal constituent with an amplitude distribution across the boundary given by that of the $M_2$ constituent interpolated from the same model (Serhadlıoğlu et al., 2013). The DG ADCIRC modelling parameters were set as constant throughout the study: most of them were attained as the default values recommended by the ADCIRC model developers, and some are the same as those in the study of Serhadlıoğlu et al. (2013). The rest, such as time step, bottom friction, wetting, and drying, were determined by using equations and a parameter sensitivity analysis for the area of focus. Initially, the simulations were run without any meteorological input, in order to observe the general flow of tides through the region.

## RESULTS AND DISCUSSION

### Model Calibration

To achieve the most accurate results, the model was tuned by adjusting the quadratic bottom friction coefficient ($c_f$) until the model-predicted and observed $M_2$ tidal elevations and phases were in close agreement. The observational data were from the United Kingdom and Ireland Admiralty tide tables. The final results for fourteen calibration sites are summarized in Table 2. The computed $M_2$ phases at both ends of the ocean boundary (Stackpole Quay and Port Isaac) show a 4°–7° shift from the observed values. Therefore the computed phases that are approximately 5° larger than the observed values should be the best fit for model calibration. It is seen from Table 2 that the model results show good agreement with the observed data when using a bed friction coefficient $c_f = 0.004$. However, this estimation is an average for the entire area and does not reflect real spatial variability in frictional forces.

### Quarter-Wave Tidal Resonance

Looking ahead, the response of the system using the natural forcing frequency ($\omega/\omega_{M_2} = 1.0$), it is found that the dominant frequency of the Bristol Channel response is larger than the natural frequency (Figs. 3–7), which indicates that the basin length of the Bristol Channel is shorter than the quarter wavelength required for resonance. This is consistent with the result if we compare the $M_2$ quarter wavelength with the length of the Bristol Channel. Tidal waves in the Bristol Channel behave as "long waves" since their wavelength is much greater than the water depth, implying that vertical motion may be neglected. The wavelength of a shallow wave is given by the formula below:

$$L = \frac{2\pi\sqrt{gH}}{\omega} \tag{4}$$

where $g$ is the gravitational acceleration ($ms^{-2}$), $H$ is the water depth (m), and $\omega$ is the angular frequency of the tidal component (radians $s^{-1}$) (Godin, 1993). If we take $H \approx 40$ m for the Bristol Channel, since $\omega = 1.405 \times 10^{-4} s^{-1}$ for the constituent $M_2$, we find $\frac{1}{4}L = 221$ km for the Bristol Channel. This model shows that the length of the Bristol Channel is approximately 160 km, therefore somewhat shorter than an $M_2$ quarter wavelength. The tidal resonance theory indicates that the ocean basin must satisfy the well-known quarter-wavelength requirement. Godin (1993) found that the restricted concept was a necessary but not sufficient condition for the phenomenon to occur, especially for deeper embayments. Serhadlıoğlu (2014) found that the Bristol Channel is shorter than the quarter wavelength for the $M_2$ tidal period. The results presented here agree with this finding and suggest that the quarter-wavelength requirement may become more relaxed for shallow basins.

**Resonant Periods**

The $M_2$ response curves of the Bristol Channel have been investigated by exciting the model using artificially altered $M_2$ forcing frequencies ($\omega$), and applying a ratio ($\omega/\omega_{M_2}$) varying between 0.5175 and 5.175 but with the same driving amplitude at the outer boundary. The simulated results of $M_2$ elevations were sampled at 16 model stations along the Bristol Channel and at 5 stations across the midchannel (Fig. 2). Station C is overlapped with ST11.

The response curves of several stations taken along the Bristol Channel are plotted in Fig. 3, in which four stations (ST3, ST5, ST7, and ST9) represent the inner section of the Bristol Channel while three stations (ST11, ST13, and ST15) represent the outer channel. In Fig. 3, the response curves follow a similar pattern at all of the stations considered but differ in magnitude because of

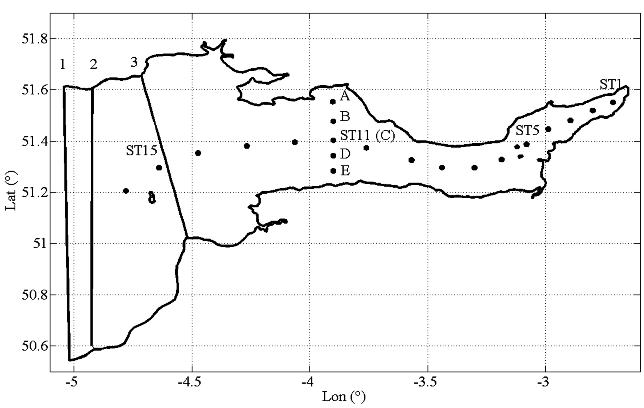


Fig. 2 Sixteen stations along the Bristol Channel and five stations along the midchannel with boundaries 1, 2, and 3 from left to right (with the original boundary being boundary 2)

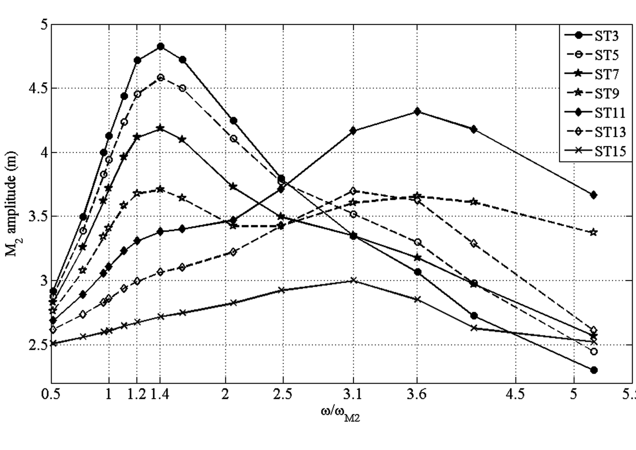


Fig. 3 Response curves of several stations (ST3, ST5, ST7, and ST9) along the Bristol Channel represent the inner channel while ST11, ST13, and ST15 represent the outer channel.

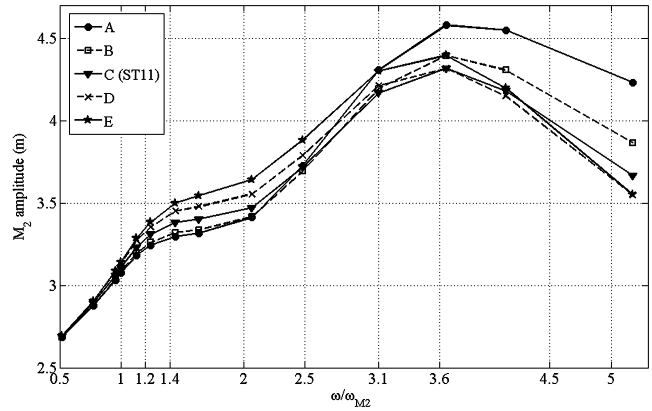


Fig. 4 Response curves of stations across the midchannel near Swansea Bay

the location of the model station. It is shown that all of the stations show a peak in response at a ratio of approximately 1.2–1.4, which indicates the quarter-wavelength resonance of the system with a period of approximately 8.87–10.35 hours. A second peak is observed at $\omega/\omega_{M_2} = 3.1$–$3.6$ in the outer channel, and the peak variation is seen to be very site-dependent. Equation 4 suggests that this may be a resonance occurring at the channel entrance.

Figure 4 shows the response curves of all five of the stations across the midchannel. At the forcing frequency of approximately $\omega/\omega_{M_2} = 3$–$4$ there is a significant increase in the $M_2$ amplitude response. When approaching the coasts, the response slightly increases, which is probably because of the decrease in water depth. The increase of response amplitudes at Stations A and B is more obvious: this may be attributed to the topography of the coast near them compared to the other side.

The resonant period calculated from the model results is within the range suggested by previous studies, which suggested a resonant period between 7.3 and 11.3 hours (Table 1). The method used in this study was the same as that of Serhadlıoğlu (2014), but the dominant tidal period obtained here is slightly lower than in that study. This subtle difference might be due to the coupled nature of two different modelling systems, and this reason was also suggested by Serhadlıoğlu (2014). In the present study the model domain only includes the Bristol Channel, while in Serhadlıoğlu's study (Serhadlıoğlu, 2014) the Irish Sea, Celtic Sea, English Channel, and Bristol Channel are all included. Table 1 also indicates that when the Celtic Sea is included in the model the resonant period is likely to be larger compared to that only including the Bristol Channel. Additionally, the present model applies a coarser mesh than that in Serhadlıoğlu (2014). These may both contribute to the peak shift of the resonant response.

Figure 5 illustrates the amplification of the response along the Bristol Channel by normalising the response of the Bristol Channel by the elevation at the channel mouth (solid line). Figure 5 also shows the amplification within the inner channel and in the outer channel. The inner section of the Bristol Channel shows an amplified response over the frequency range $\omega/\omega_{M_2}$ ratio of 1.2–1.5 (dashed line) while the outer channel exhibits an apparent resonance around the ratio of 4.1 (dotted line). The result indicates a coupled resonant system of the Bristol Channel: the main peak might be the dominant resonant mode ($\omega/\omega_{M_2} = 1.3$) of the Bristol Channel, while the second peak ($\omega/\omega_{M_2} = 4.1$) might be due to the response of the channel to the forcing at its mouth. This complicated resonance pattern was also found by Liang et al. (2014). They suggested that some regions in the outer Bristol Channel

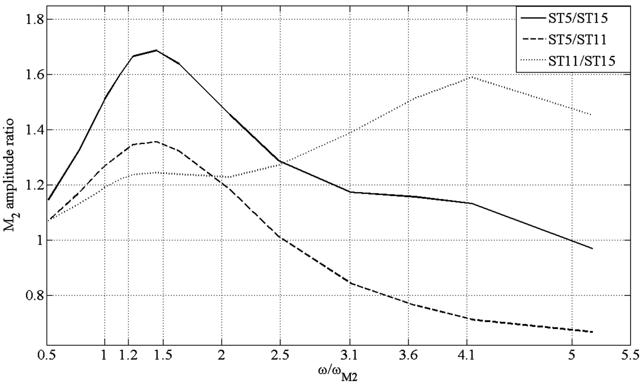


Fig. 5 Amplification of the response observed in the channel

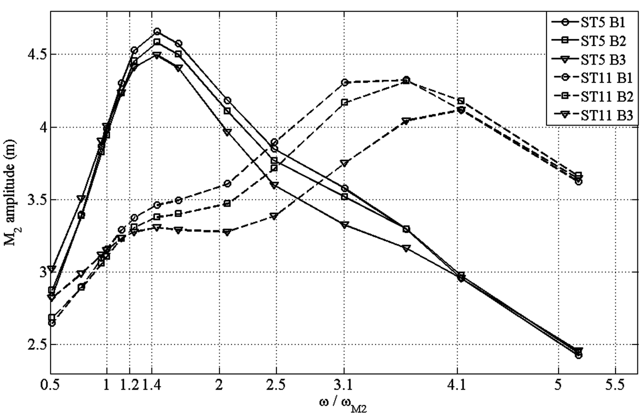


Fig. 6 Response curves of ST5 and ST11 with different boundary positions

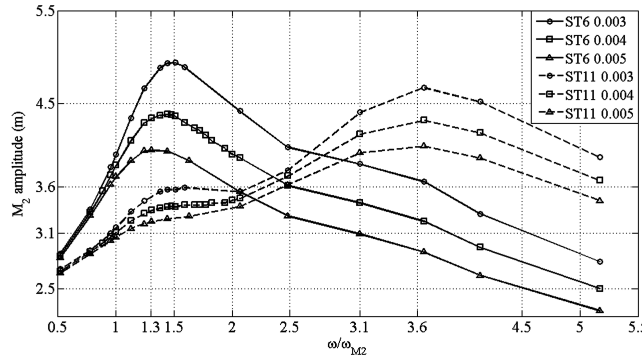


Fig. 7 Response curves of ST6 and ST11 with different bed frictions

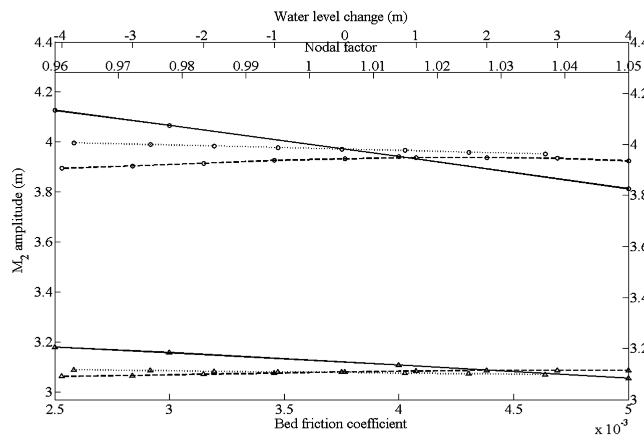


Fig. 8 Sensitivity test results on water level (dashed lines), nodal factor (dotted lines), and bed friction (solid lines) at ST5 (lines with circular markers) and ST11 (lines with triangular markers)

also experience significant, if not greater, resonances when the $\omega/\omega_{M_2}$ ratio lies in the range of 3–6.

Figure 6 presents the comparison of $M_2$ response curves obtained from the models with three different boundary positions (shown in Fig. 2). Boundary 2 is the original one adopted in this study. It is seen that the peak at approximately $\omega/\omega_{M_2} = 1.2$–$1.4$ is not shifted with the changing boundary position, while the second peak is apparently boundary-dependent because it is shifted from a ratio of approximately 3.1 to approximately 4.1 with the boundary moving up to the channel head. This again indicates that the second peak should be the tidal response with the open boundary at the outer channel. It is also worth noting that the response amplitudes decrease with the boundary position moving from the ocean to the channel head. Therefore, in the present study, the dominant resonant mode of the $M_2$ response in the Bristol Channel is hardly affected by the slight changing of boundary position.

The Bristol Channel is a complex hydrodynamic system and sensitive to small changes. Factors such as bed friction can have influences on the resonant period. As seen in Fig. 7, it is obvious that the amplitudes of $M_2$ response curves drop with an increasing bed friction coefficient. However, we also find that the bed friction can affect the resonant period since a shift of the peak can be seen from a ratio of $\omega/\omega_{M_2} = 1.3$ to $\omega/\omega_{M_2} = 1.5$ in the inner Channel (ST6). There is a great deal of interest in extracting energy from the Bristol Channel, and adding bottom friction would be a simplistic representation of modelling this. This implies that the impact of resonances on the channel should be taken into account by tidal energy development.

## Sensitivity Tests

The results of the sensitivity tests on water level, 18.6-year nodal cycle, and bed friction in both inner (ST5) and outer (ST11) parts of the channel are shown in Fig. 8. The response tides are driven by the tidal forcing of the $M_2$ constituent.

Sea level rise (SLR) is the dominant influence on any far-field impacts and has influenced the tidal regimes in the past. Some modelling studies show that even moderate SLR may have significant impact on the tides on the European shelf (Ward et al., 2012). In the present study, however, with water level varying from 4 m lower to 4 m higher than the real situation, the tidal heights do not present visible change in the Bristol Channel. The angle between the plane of the Moon's orbit around the Earth and the plane through the equator of the Earth varies with a period of 18.6 years, and the nodal tidal cycle is usually represented as a linear modulating factor in the calculation of the tidal amplitudes (Adcock et al., 2014). Thus, for the $M_2$ constituent:

$$\eta_{M_2} = f_{M_2} \times a_{M_2} \cos(\omega_{M_2} t + \phi) \qquad (5)$$

where $\eta_{M_2}$ is the water level variation at the frequency of $M_2$, $f_{M_2}$ is the nodal factor, $a_{M_2}$ is the amplitude of the $M_2$ constituent, $\omega_{M_2}$ is the frequency of the $M_2$ tide, and $\phi$ is its phase. $M_2$ was the only tidal constituent used in this model; therefore, $f_{M_2}$ dominates the annual water-level variation. Over a period of 9.3 years, the $M_2$ nodal factor changes from its minimum value of 0.96 to its maximum value of 1.04; however, during this time period the relative response of the $M_2$ tidal heights remains almost unchanged. This suggests that the response is essentially linear over the range of interest.

The bed friction is seen to be the dominant effect on the tidal response, since the $M_2$ amplitude at ST11 decreases by approximately 0.2 m with the quadratic friction coefficient increasing from 0.0025 to 0.005; and the bed friction is found to have greater influence on the shallower areas. Tidal amplitude is strongly affected by frictional resistance, especially in shallow channels. In nature the forced resonant oscillations cannot grow indefinitely because the leakage of energy due to friction increases more rapidly than the amplitudes of the oscillations. When friction is incorporated, the progressive waves are damped so that the elevation decreases with distance in the wave propagation direction, and the reflected waves may also travel along with lower amplitudes.

**Response to Disturbances**

An alternative approach to investigating the resonant frequency is to examine the response to disturbances. In this case we apply a shear stress, which can be thought of as surface forcing due to wind, and examine the subsequent oscillations once the wind is removed. Simulations were run with winds blowing over the whole model domain from five different directions: south, southwest, west, northwest, and north. The wind applied here is created by using MATLAB code and varies linearly with time. In this section the modelling area (Fig. 9) includes not only the Bristol Channel, but also the Celtic Sea, the Irish Sea, and the English Channel, which is the same model used in Serhadlıoğlu's study (Serhadlıoğlu, 2014). Five locations in the upper channel (Avonmouth, Hinkley Point, Newport, Ilfracombe, and Mumbles) were selected as the model sites (Fig. 1). We simulate storms normally lasting 2 days (Days 7 and 8), during which the wind is 30 ms$^{-1}$.

On Day 9 the southerly winds stops, but it is seen in Fig. 10 that the surge overshoots and becomes negative. From Day 10 the residuals display the development of oscillations with a similar period and heights ranging from approximately −0.2 m to 0.2 m in all five of the sites. It takes approximately four days for the oscillations to decay. An explanation for the development of such oscillations would be that the system is freely resonating.

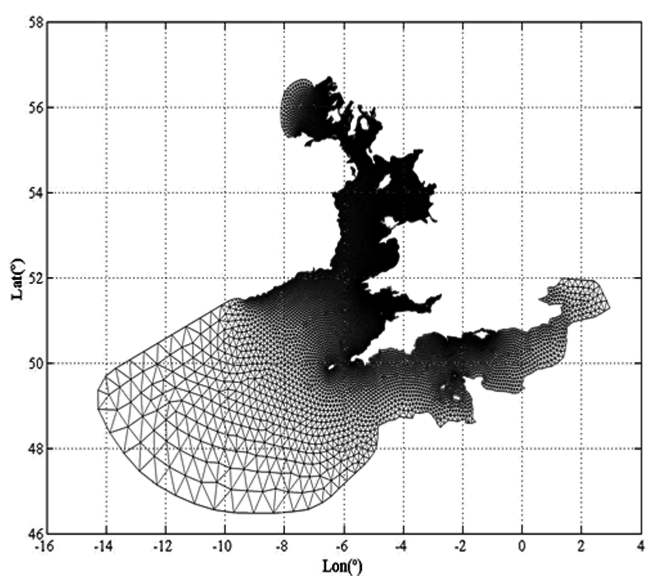


Fig. 9 Model mesh including the Irish Sea, Celtic Sea, English Channel, and Bristol Channel

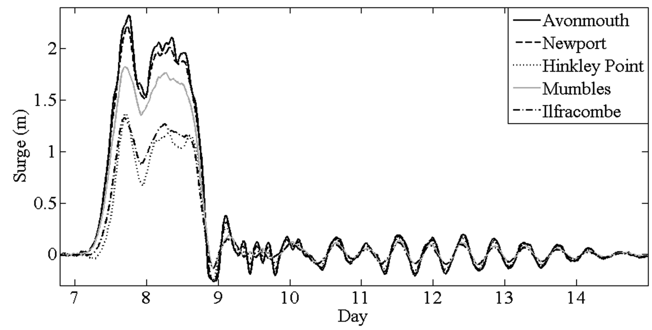


Fig. 10 Residuals calculated at five stations: repetitive oscillations can be seen at all five stations after southerly winds stopped running.

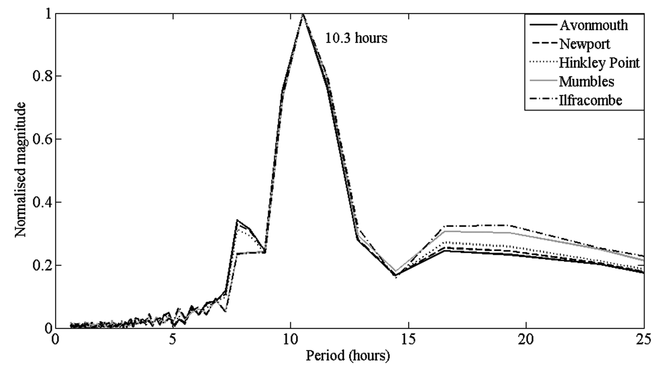


Fig. 11 Normalised magnitude spectrum over a period of 11 surge with southwesterly winds imposed at five sites

A fast Fourier transform (FFT) was used to analyse the frequencies present in the signal. Surge data from Day 11 to Day 14 (Fig. 10) was taken for FFT analysis. Figure 11 shows the normalised amplitude spectrum by the peak response over a period of surges that resulted from southwesterly winds in the channel. A dominant peak can be seen that indicates the dominant oscillation period of approximately 10.3 hours. Similar results occurred when winds from different directions were used.

This matches the resonance period of the Bristol Channel found in this study (8.87–10.35 hours). The resonant periods of 7.8 hours and 17 hours are also found, but the cause is unclear. Webb (2013) investigated the resonances of the English Channel and Irish Sea by running the model, based on the shallow water equations, at angular frequencies between 0 and 30 radians per day. The modelling results showed that the key resonant period is between 10.8 and 11.6 hours. Webb (2013) also found that the amplitude responses peaked between 5 and 8 hours; however, these modes have a more complicated structure, and it was more difficult to relate the modes to specific physical features of the system. To conclude, the results in Fig. 11 indicate that the Bristol Channel is a coupled resonance system with a dominant resonant period of 10.3 hours. This is in close agreement with Webb (2013), Liang et al. (2014), and Serhadlıoğlu (2014), which suggested a coupled resonance system in the Bristol Channel.

## CONCLUSIONS

Two 2-D shallow-water models were used to study the tidal resonance in the Bristol Channel. The results from simulations with tide alone and wind alone show that the quarter-wavelength resonant period of the Bristol Channel has a coupled resonance system with a dominant resonant period of 8.87–10.35 hours and 10.3 hours, respectively. This is close to but shorter than the semidiurnal tidal band, suggesting that the basin length of the Bristol Channel is shorter than the resonant quarter wavelength. Generally speaking, the main resonance of the Bristol Channel seems consistent with previous studies, and the second peak at approximately $\omega/\omega_{M_2} = 3.1$ might be the resonant response of the outer channel itself; the causes for the resonant periods of 7.8 hours and 17 hours found during wind disturbance simulations are unclear, and future investigation is needed. The main resonance is slightly sensitive to increased bed friction, which may have implications for tidal energy extraction. Neither the amplitude on the boundary nor the mean water level has a significant impact on the resonant response, suggesting that the nodal factor of the tide, or any possible sea-level rise, will not dramatically influence the tidal response in the channel.

## ACKNOWLEDGEMENTS

We are grateful to Dr. Sena Serhadlıoğlu, who carried out a preliminary study of this topic in her Ph.D. (DPhil) project at the University of Oxford. She has also been a great support throughout the first year of this study.

## REFERENCES

Adcock, TAA, Draper, S, and Nishino, T (2015). "Tidal Power Generation: A Review of Hydrodynamic Modelling," *Proc Inst Mech Eng*, *Part A*, 229(7), 755–771. https://doi.org/10.1177/0957650915570349.

Adcock, TAA, Draper, S, Houlsby, GT, Borthwick, AGL, and Serhadlıoğlu, S (2014). "Tidal Stream Power in the Pentland Firth: Long-Term Variability, Multiple Constituents, and Capacity Factor," *Proc Inst Mech Eng*, *Part A*, 228(8), 854–861. https://doi.org/10.1177/0957650914544347.

Baker, C (1991). "Tidal Power," *Energy Policy*, 19(8), 792–797. https://doi.org/10.1016/0301-4215(91)90049-T.

Bondi, H (1981). *Tidal Power from the Severn Estuary, Vol. 1*, Report to the Secretary of State for Energy prepared by the Severn Barrage Committee.

Falconer, RA (1993). "An Introduction to Nearly Horizontal Flows," *Coastal, Estuarial and Harbor Engineers Reference Book*, CRC Press, 27–36.

Fong, SW, and Heaps, NS (1978). *Note on Quarter Wave Tidal Resonance in the Bristol Channel*, IOS Report 63, Bidston Observatory, Birkenhead, Institute of Oceanographic Sciences, 11 pp.

Godin, G (1993). "On the Tidal Resonance," *Cont Shelf Res*, 13(1), 89–107. https://doi.org/10.1016/0278-4343(93)90037-X.

Google Earth 7.1.7.2606 (2016). http://www.earth.google.com (accessed October 6), 51°03'02.37"N, 3°50'40.98"W, eye alt 199.53 km, Landsat/Corpernicus.

Hashemi, MR, Abedini, MJ, Neill, SP, and Malekzadeh, P (2008). "Tidal and Surge Modelling Using Differential Quadrature: A Case Study in the Bristol Channel," *Coastal Eng*, 55(10), 811–819. https://doi.org/10.1016/j.coastaleng.2008.02.030.

Heath, R (1981). "Resonant Period and Q of the Celtic Sea and Bristol Channel," *Estuarine Coastal Shelf Sci*, 12(3), 291–301. https://doi.org/10.1016/S0302-3524(81)80126-0.

Kubatko, EJ, Westerink, JJ, and Dawson, C (2006). "hp Discontinuous Galerkin Methods for Advection Dominated Problems in Shallow Water Flow," *Comput Methods Appl Mech Eng,* 196(1–3), 437–451. https://doi.org/10.1016/j.cma.2006.05.002.

Liang, D, Xia, J, Falconer, RA, and Zhang, J (2014). "Study on Tidal Resonance in Severn Estuary and Bristol Channel," *Coastal Eng J*, 56(01), 1450002. https://doi.org/10.1142/S0578563414500028.

Marmer, HA (1922). "Tides in the Bay of Fundy," *Geog Rev*, 12(2), 195–205. https://doi.org/10.2307/208736.

Pugh, D, and Woodworth, P (2014). *Sea-Level Science: Understanding Tides, Surges, Tsunamis and Mean Sea-Level Changes*, Cambridge University Press, 407 pp.

Pugh, DT (1996). *Tides, Surges and Mean Sea Level: A Handbook for Engineers and Scientists* (reprinted with corrections), John Wiley & Sons, 486 pp.

Robinson, I (1980). "Tides in the Bristol Channel: An Analytical Wedge Model with Friction," *Geophys J Int*, 62(1), 77–95. https://doi.org/10.1111/j.1365-246X.1980.tb04845.x.

Serhadlıoğlu, S (2014). *Tidal Stream Resource Assessment of the Anglesey Skerries and the Bristol Channel*, PhD (DPhil) Thesis, University of Oxford, Oxford, UK.

Serhadlıoğlu, S, Adcock, TAA, Houlsby, GT, Draper, S, and Borthwick, AGL (2013). "Tidal Stream Energy Resource Assessment of the Anglesey Skerries," *Int J Mar Energy*, 3–4, e98–e111. https://doi.org/10.1016/j.ijome.2013.11.014.

Ward, SL, Green, JM, and Pelling, HE (2012). "Tides, Sea-Level Rise and Tidal Power Extraction on the European Shelf," *Ocean Dyn*, 62(8), 1153–1167. https://doi.org/10.1007/s10236-012-0552-6.

Webb, DJ (2013). "On the Shelf Resonances of the English Channel and Irish Sea," *Ocean Sci*, 9(4), 731–744. https://doi.org/10.5194/os-9-731-2013.

Willis, M, et al. (2010). "Tidal Turbine Deployment in the Bristol Channel: A Case Study," *Proc Inst Civil Eng Energy*, 163(3), 93–105. https://doi.org/10.1680/ener.2010.163.3.93.

Xia, J, Falconer, RA, Lin, B, and Tan, G (2012). "Estimation of Annual Energy Output from a Tidal Barrage Using Two Different Methods," *Appl Energy*, 93, 327–336. https://doi.org/10.1016/j.apenergy.2011.12.049.